THE PEOPLE'S DEMOCRATIC REPUBLIC OF ALGERIA
MINISTRY OF HIGHER EDUCATION AND SCIENTIFIC RESEARCH

UNIVERSITY « Dr. TAHAR MOULAY » OF SAIDA

FACULTY OF SCIENCES

PHYSICS DEPARTMENT

DISSERTATION

Presented for the graduation of

MASTER

Specialty: PHYSICS

Option: radiation Physics

By

DINE SIHEM FAKHR

On the Subject

Calculation of structural, elastic, electronic and optical properties of LiZnN : First principle study.

Defended on 09/09/2020 in front of the jury composed of :

Dr. ELKEURTI Mohammed	Pr	U . Saida	President
Dr. BOUDIA Keltouma	M.C.A	U.C .Tessemsilt	Reporter
Dr. BOUTALEB Habib	M.C.B	U . Saida	Co- Reporter
Dr. KHELEFAOUI Friha	M.C.B	U . Saida	Examiner

Session 2019 – 2020

Dedication

Above all I would like to thank the almighty ALLAH, the lord of the universe, my creator, my strong pillar, my source of inspiration, wisdom, knowledge and understanding. For all the strength and perseverance he has installed in me during all the years of my studies, without him this work wouldn't have been started. We will always be in the shelter of ALLAH from now and until hereafter life. Amine.

This work is dedicated to my beloved parents DINE Ahmed and Naouel, who have been my source of inspiration and gave me strength, and who continually provide their moral, spiritual, emotional, and financial support.

To my husband MOGHERBI Adnane, Uncle DINE Khaled ,brother DINE Faiçal, sisters Manel and Samar, my son Wassim.

To my relatives, mentor, friends, and classmates who shared their words of advice and encouragement.

ACKNOWLEDGEMENT

First and foremost, praises and thanks to Allah for his showers of blessings throughout my research work to complete the research successfully.

I would first like to thank my master thesis Reporter BOUDIA Keltouma and my Co-Reporter Dr. BOUTALEB Habib, for all their help and guidance that they have given me over the past six months. You have set an example of excellence as a researcher, mentor, instructor, and role model.

I would also like to thank the jury members Dr. KHELEFAOUI Friha and Dr. ElKEURTI Mohammed for accepting to evaluate this work.

I would also like to acknowledge all my teachers of department of physics especially Dr. LABANI Fatima.

I would especially like to thank my family for the love, support, and constant encouragement I have gotten over the years. In particular, I would like to thank my parents, my husband, my uncle, my brother, my two lovely sisters, my son; I undoubtedly could not have done this without you.

Last but not least, deepest thanks go to all people who took part in making this thesis real.

Table of contents

List of Figures:

List of Tables:

General Introduction

General introduction:

Unlike the majority of electronic devices, which are silicon based, optoelectronic devices are predominantly made using III–V semiconductor compounds such as GaAs, InP, GaN, and GaSb, and their alloys due to their direct-band gap. Understanding the properties of these materials has been of vital importance in the development of optoelectronic devices. Since the first demonstration of a semiconductor laser in the early 1960s, optoelectronic devices have received considerable attention due to their applications in communications, computing, entertainment, lighting, and medicine.

II–VI semiconductors have attracted much interest in fundamental research in various areas. For example, the study of diluted magnetic semiconductor (DMS) and manganese-based alloys[1], the emission of single photons in the visible range with CdSe quantum boxes [2], or Bose condensation of excitants in CdTe-based microcavities [3] or again Aharonov–Bohm effect[4]. II–VI semiconductors, such as ZnS, ZnSe and CdTe, appear to be promised for optoelectronic applications [5-15]. The limitation of some II–VI semiconductors in various fields makes the search of new semiconductors a major challenge for materials science. The first work on the chalcopyrites was carried out by Hahn et al.[16]; later, studies on this family of compounds have been largely motivated by their potential in different applications. The similarity between the zinc-blende and chalcopyrite structure has pushed the scientists to focus their attention on this compounds family. Effectively, Zunger and his collaborators [17, 18] have explained the formation of ternary compounds made by a substitution of atoms in a tetrahedral empty site. Another particularly interesting class of materials is named half-Heusler compounds or ‘‘Nowotny– Juza,’’ [19] with a chemical composition XYZ. So, the half-Heusler compounds, which have eight valence electrons, including a large number of semiconductors with energy gaps vary in a wide range [20]. In general, the half-Heusler materials with eight valence electrons can be of II–VI, I–II V, I–III– IV, II–II–IV and III–II–III type. In addition, the

ferromagnetic behavior was observed by de Groot et al. [21] in half-Heusler compounds. Researchers have resumed the studies on these materials that can show: the topological properties [22-24] , they can also be used as spintronic devices [25] and as thermo-electrics with high-performance [26-28]. Recently, Roy et al have predicted the piezoelectric response and their associated properties in half-Heusler compounds. Another significant theoretical advancement came in 1985, and first principle calculations were presented by Wood et al.[17] who have predicted the energy gaps of about 1 eV in Li–half-Heusler compounds. After experimental and theoretical observations [29, 30]on the NiSnZr half-Heusler, a lot of additional semiconductor systems have been identified [20, 31, 32] . Some of these compounds, such as LiMgN and LiMgP, have large energy gaps that make them suitable for optoelectronic applications [33-35].

The properties of the Nowonty-Juza phases are strongly determined by their crystalline order and the resulting electronic structure. Particularly, the electronic structures of LiMgN and LiZnN were proposed to fill the green gap left open by existing InGaN-based emission devices[36].Most of NaMgZ (Z = N, P, As, Sb and Bi) compounds have been theoretically predicted as direct band gap materials. Ab initio calculations show that both NaMgP and NaMgN are potential candidates for light-emitting diodes [37].

KMgZ (Z = N, P, As, Sb and Bi) compounds crystallize in zinc blende structure (space group F-43m). Theoretically, the KMgN is found to have an indirect band gap of 0.13 eV [38], whereas KMgP, KMgAs and KMgSb are found to have direct band gaps of 0.96, 0.46 [37] and 0.59 eV, respectively [39].

In this work, we report on first principles calculations of the structural, elastic, electronic and optical properties of our compounds LiZnN, which is organized as follows:

- The first chapter is devoted to present general information on heusler alloys as well as their nomenclature, their crystal structure within order and disorder phenomena and their application.
- The second and the last chapter, is devoted to present and discuss the obtained results, their interpretations as well as a comparison with some theory and experimental works of our compound.
- Finally, a brief conclusion is given about the obtained results.

Bibliography:

1. Furdyna, J.K., *Diluted magnetic semiconductors.* Journal of applied physics, 1988. **64**(4): p. R29-R64.
2. Sebald, K., et al., *Single-photon emission of CdSe quantum dots at temperatures up to 200 K.* Applied physics letters, 2002. **81**(16): p. 2920-2922.
3. Kasprzak, J., et al., *Bose–Einstein condensation of exciton polaritons.* Nature, 2006. **443**(7110): p. 409-414.
4. Sellers, I., et al., *Aharonov-Bohm excitons at elevated temperatures in type-II ZnTe/ZnSe quantum dots.* Physical review letters, 2008. **100**(13): p. 136405.
5. Jiang, X., et al., *Simultaneous in situ formation of ZnS nanowires in a liquid crystal template by γ-irradiation.* Chemistry of Materials, 2001. **13**(4): p. 1213-1218.
6. Elidrissi, B., et al., *Structure, composition and optical properties of ZnS thin films prepared by spray pyrolysis.* Materials Chemistry and physics, 2001. **68**(1-3): p. 175-179.
7. Yamaga, S., A. Yoshikawa, and H. Kasai, *Electrical and optical properties of donor doped ZnS films grown by low-pressure MOCVD.* Journal of crystal growth, 1988. **86**(1-4): p. 252-256.
8. Falcony, C., et al., *Luminescent properties of ZnS: Mn films deposited by spray pyrolysis.* Journal of applied physics, 1992. **72**(4): p. 1525-1527.
9. Prevenslik, T., *Acoustoluminescence and sonoluminescence.* Journal of Luminescence, 2000. **87**: p. 1210-1212.
10. Xu, C.-N., et al., *Preparation and characteristics of highly triboluminescent ZnS film.* Materials research bulletin, 1999. **34**(10-11): p. 1491-1500.
11. Tang, W. and D. Cameron, *Electroluminescent zinc sulphide devices produced by sol-gel processing.* Thin Solid Films, 1996. **280**(1-2): p. 221-226.
12. Basol, B.M., *Electrodeposited CdTe and HgCdTe solar cells.* Solar Cells, 1988. **23**(1-2): p. 69-88.
13. Lischka, K., *Epitaxial ZnSe and Cubic GaN: Wide-Band-Gap Semiconductors with Similar Properties?* physica status solidi (b), 1997. **202**(2): p. 673-681.
14. Ando, K., et al., *Highly Efficient Blue–Ultraviolet Photodetectors Based on II–VI Wide-Bandgap Compound Semiconductors.* physica status solidi (b), 2002. **229**(2): p. 1065-1071.
15. Ma, C., et al., *Nanobelt and nanosaw structures of II-VI semiconductors.* International journal of nanotechnology, 2004. **1**(4): p. 431-451.
16. Hahn, H., et al., *Anorg.* AlIg, Chern, 1953. **271**: p. 153.
17. Wood, D., A. Zunger, and R. De Groot, *Electronic structure of filled tetrahedral semiconductors.* Physical Review B, 1985. **31**(4): p. 2570.
18. Wei, S.-H. and A. Zunger, *Electronic structure and phase stability of LiZnAs: A half ionic and half covalent tetrahedral semiconductor.* Physical review letters, 1986. **56**(5): p. 528.
19. Nowotny, H. and K. Bachmayer, *Die Verbindungen LiMgP, LiZnP und LiZnAs.* Monatshefte für Chemie und verwandte Teile anderer Wissenschaften, 1950. **81**(4): p. 488-496.
20. Kandpal, H.C., C. Felser, and R. Seshadri, *Covalent bonding and the nature of band gaps in some half-Heusler compounds.* Journal of Physics D: Applied Physics, 2006. **39**(5): p. 776.
21. De Groot, R., et al., *New class of materials: half-metallic ferromagnets.* Physical review letters, 1983. **50**(25): p. 2024.
22. Chadov, S. and X. Qi, *J. Kü bler, GH Fecher, C. Felser, SC Zhang.* Nat. Mater, 2010. **9**: p. 541.
23. Lin, H., et al., *Nature Mater. 9, 546 (2010).*
24. Zhang, H.-J., et al., *Topological insulators in ternary compounds with a honeycomb lattice.* Physical review letters, 2011. **106**(15): p. 156402.
25. Felser, C., G.H. Fecher, and B. Balke, *Spintronics: a challenge for materials science and solid-state chemistry.* Angewandte Chemie International Edition, 2007. **46**(5): p. 668-699.
26. Shen, Q., et al., *Effects of partial substitution of Ni by Pd on the thermoelectric properties of ZrNiSn-based half-Heusler compounds.* Applied physics letters, 2001. **79**(25): p. 4165-4167.
27. Nolas, G.S., J. Poon, and M. Kanatzidis, *Recent developments in bulk thermoelectric materials.* MRS bulletin, 2006. **31**(3): p. 199-205.
28. Balke, B., et al., *An alternative approach to improve the thermoelectric properties of half-Heusler compounds.* Journal of electronic materials, 2011. **40**(5): p. 702-706.
29. Ślebarski, A., et al., *Electronic structure of X 2 ZrSn-and X ZrSn-type Heusler alloys with X= Co or Ni.* Physical Review B, 1998. **57**(11): p. 6408.
30. Öğüt, S. and K.M. Rabe, *Band gap and stability in the ternary intermetallic compounds NiSnM (M= Ti, Zr, Hf): A first-principles study.* Physical Review B, 1995. **51**(16): p. 10443.
31. Kieven, D., et al., *I-II-V half-Heusler compounds for optoelectronics: Ab initio calculations.* Physical Review B, 2010. **81**(7): p. 075208.

32. Gruhn, T., *Comparative ab initio study of half-Heusler compounds for optoelectronic applications.* Physical Review B, 2010. **82**(12): p. 125210.
33. Casper, F., R. Seshadri, and C. Felser, *Semiconducting half-Heusler and LiGaGe structure type compounds.* physica status solidi (a), 2009. **206**(5): p. 1090-1095.
34. Kuriyama, K., K. Nagasawa, and K. Kushida, *Growth and band gap of the filled tetrahedral semiconductor LiMgN.* Journal of crystal growth, 2002. **237**: p. 2019-2022.
35. Kuriyama, K., K. Kushida, and R. Taguchi, *Optical band gap of the ordered filled-tetrahedral semiconductor LiMgP.* Solid state communications, 1998. **108**(7): p. 429-432.
36. Walsh, A. and S.-H. Wei, *Theoretical study of stability and electronic structure of Li (Mg, Zn) N alloys: A candidate for solid state lighting.* Physical Review B, 2007. **76**(19): p. 195208.
37. Mehnane, H., et al., *First-principles study of new half Heusler for optoelectronic applications.* Superlattices and Microstructures, 2012. **51**(6): p. 772-784.
38. Charifi, Z., et al., *Phase transition of Nowotny–Juza NaZnX (X= P, As and Sb) compounds at high pressure: Theoretical investigation of structural, electronic and vibrational properties.* Computational Materials Science, 2014. **87**: p. 187-197.
39. Bennett, J.W., et al., *Hexagonal A B C semiconductors as ferroelectrics.* Physical review letters, 2012. **109**(16): p. 167602.

Chapter I

Heusler Alloys

I.1 Introduction:

Heusler compounds are ternary intermetallics permitting the prediction of half-metallic semiconductors, and superconductors [1]. There are two families of Heusler compounds: half-Heusler compounds *XYZ*, and (full) Heusler compounds XY_2Z and crystallize in crystalline cubic structure. Today Heusler compounds form a large class of more than 3000 compounds that exhibit versatile properties. Figure.I.1 shows an over view of possible combinations of elements forming these materials.

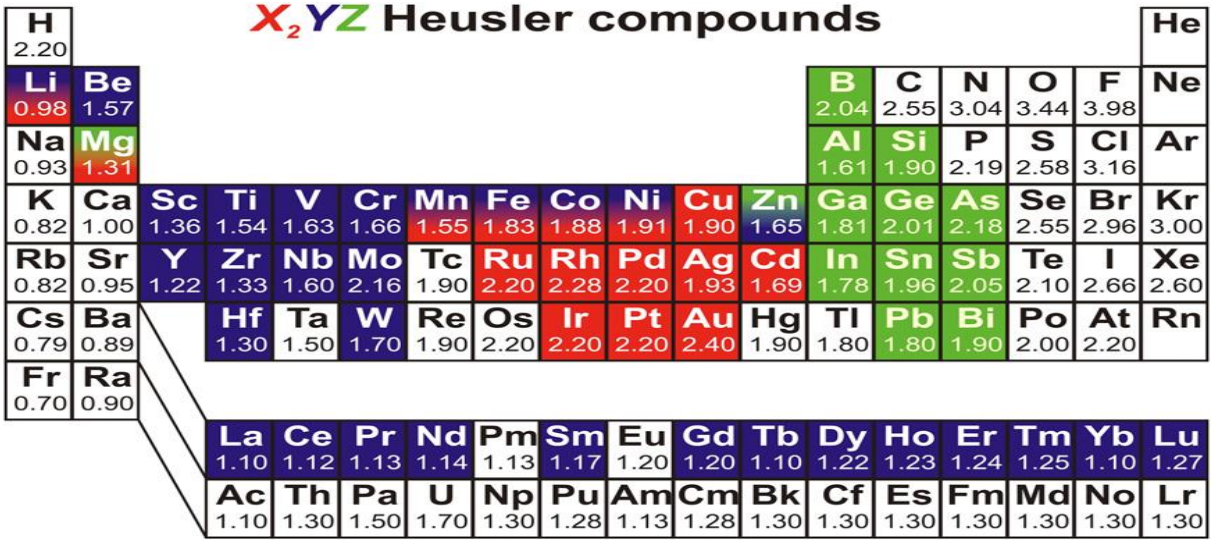

***Figure I.1**: Periodic table of the elements. The huge number of Heusler materials can be formed by combination of the different elements according to the color scheme [2].*

I.2 Nomenclature of Heusler compounds:

I.2.1. Half-Heusler compounds:

In general, Half-Heusler materials XYZ can be understood as compounds consisting of a covalent and an ionic part. The X and Y atoms have a distinct cationic character, whereas Z can be seen as the anionic counterpart [3, 4]. The nomenclature in literature varies a lot, ranging from sorting the elements alphabetically, according to their electro-negativity or randomly, and thus, all three possible permutations can be found. In this work, we will stick to an order reflecting the

electro-negativity. The most electropositive element is placed at the beginning of the formula. It can be a main group element, a transition metal or a rare earth element. The most electronegative element, at the end, is a main group element from the second half of the periodic table, e.g. LiAlSi, ZrNiSn, LuAuSn [5-7]

I.2.2. Full-Heusler compounds:

In the past, Heusler compounds were often understood as inter-metallic alloys, although the description as an inter-metallic compound is more appropriate due to their characteristic atomic order. Ternary Heusler compounds have the general formula X_2YZ, where X and Y are transition metals and Z is a main group element.

However, in some cases Y is replaced be a rare earth element or an alkaline earth metal. Traditionally, the metal, which exists twice, is put at the beginning of the formula, whereas the main group element is placed at the end, e.g. Co_2MnSi, Fe_2Val [8] . Exceptions are those compounds, in which one element can definitively be defined to be most electropositive, for instance $LiCu_2Sb$ and YPd_2Sb [9].

I.2.3.Quaternary Heusler compounds:

Except the usual and inverse full-Heusler compounds, another full-Heuslers family are the LiMgPdSn-type ones, also known as LiMgPdSb-type[10] Heusler compounds. These are quaternary compounds with the chemical formula XX'YZ, where X, X', and Y are transition metal atoms.

I.3 Crystal structure:

There are two distinct families of Heusler compounds according to their crystal structure and their atomic arrangements. Several properties depend on the one hand on the size difference between the involved atoms, and on the other hand on the kind of interatomic interaction, Which cause considerable changes in their magnetic and electronic properties [11].

I.3.1. Half Heusler:

I.3.1.1.Chemical Composition:

The Half-Heusler compounds with the composition 1:1:1 have the general formula XYZ and crystallize in a non-centro symmetric cubic structure (space group no. 216, F43m, $C1_b$) which is a ternary ordered variant of the CaF_2 structure and can be derived from the tetrahedral ZnS-type structure by filling the octahedral lattice sites Figure.I.2.

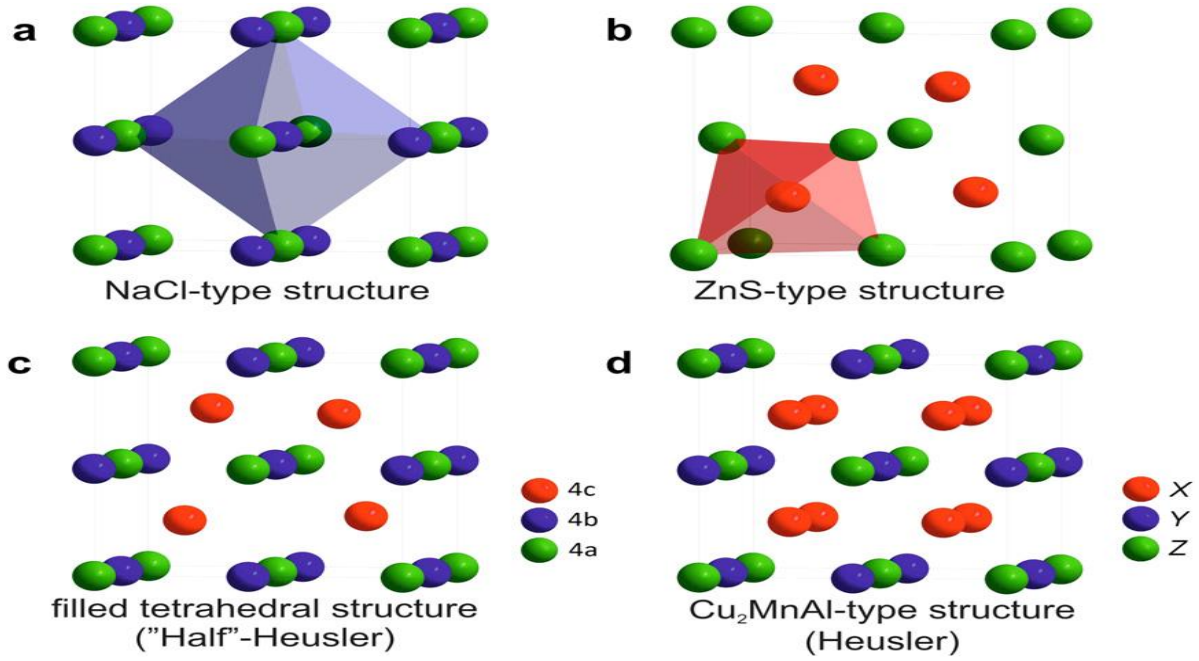

Figure I.2: *(a) Rock salt structure, (b) zinc blende structure and their relations to the Half-Heusler structure (c), and to the Heusler structure (d).*

Generally, the Half-Heusler structure type are three interpenetrating fcc sublattices, the atomic ordering according two type I and II (see TableI.1) is frequently observed. In MgAgAs Y and anionic Z form the covalent ZnS-sublattice [12], while the X and Y built the NaCl-type lattice . Consequently, As is eightfold coordinated by monovalent and divalent cations. Even though MgAgAs is the assigned prototype of all Half-Heusler compounds, it has to be clarified that this material actually crystallizes with a different atomic order than most other Half-Heusler compounds [13]. In this case a peculiar situation is present: MgCuSb [12-14] is an example which represents the atomic arrangement in most Half-Heusler materials correctly ; here, the Y

and the anionic Z form the ZnS-sublattice, and the electropositive X and the electronegative Z occupy the ionic NaCl-type sublattice.

The corresponding occupied Wyckoff positions are 4a (0, 0, 0), 4b (1/2, 1/2, 1/2), and 4c (1/4, 1/4, 1/4). In principle, three in equivalent atomic arrangements are possible within this structure type as summarized in Table.I.1.

Table I.1: In equivalent site occupancies within the C1b-type structure. Atoms on Wyckoff positions 4a and 4c form a ZnS-type sub lattice; the atoms on 4b occupy the octahedral holes.

	4a	4b	4c
I	**X**	**Y**	**Z**
II	**Z**	**X**	**Y**
III	**Y**	**Z**	**X**

I.3.1.2.Order-disorder phenomena for half- Heusler structure:

As described above, the crystal structure of materials are strongly dependent on the atomic arrangement of the atoms. Already a partial intermixture can alter the electronic structure distinctly [15]. Within the Half-Heusler structure different types of atomic disorder are possible [16] (compare Table.I.2).

Table.I.2: Site occupancy and general formula for differently ordered Half-Heusler compounds. The notations according to the Inorganic Crystal Structure Database (ICSD), the Strukturberichte (SB), the Pearson database, as well the space group are given. Wyckoff position 4d (3/4, 3/4, 3/4) denotes the second tetrahedral lattice site, which is void in ordered materials [16].

Site occupancy	General formula	Structure type ICSD	Structure type SB	Structure type Pearson	Space group
4a, 4b, 4c	XYZ	LiAlSi(MgAgAs)	$C1_b$	cF16	F43m(No. 216)
4a =4b, 4c	XZ_2	CaF2	C1	cF12	Fm3m(No. 225)
4a, 4b, 4c= 4d	X_2YZ	Cu_2MnAl	$L2_1$	cF16	Fm3m(No. 225)
4a =4b, 4c= 4d	XZ	CsCl	B2	cP2	Pm3m(No. 221)
4a =4c, 4b= 4d	YZ	NaTl	B32	cF16	Fd3m(No. 227)
4a =4b =4c= 4d	X	W	A2	cI2	Im3m(No. 229)

I.3.2.Full Heusler:

I.3.2.1.Chemical Composition:

The Heusler compounds with 2:1:1 stoichiometry, have the general formula X_2YZ and crystallize in the cubic space group Fm3m (space group no. 225) with Cu_2MnAl ($L2_1$) as prototype [17-20]. The X atoms occupy the Wyckoff position 8c (1/4, 1/4, 1/4), the Y and the Z atoms are located at 4a (0, 0, 0) and 4b (1/2, 1/2, 1/2), respectively. this structure consists of four interpenetrating fcc sublattices, two of which are equally occupied by X. A rock salt-type lattice is formed by the least and most electropositive element (Y and Z).

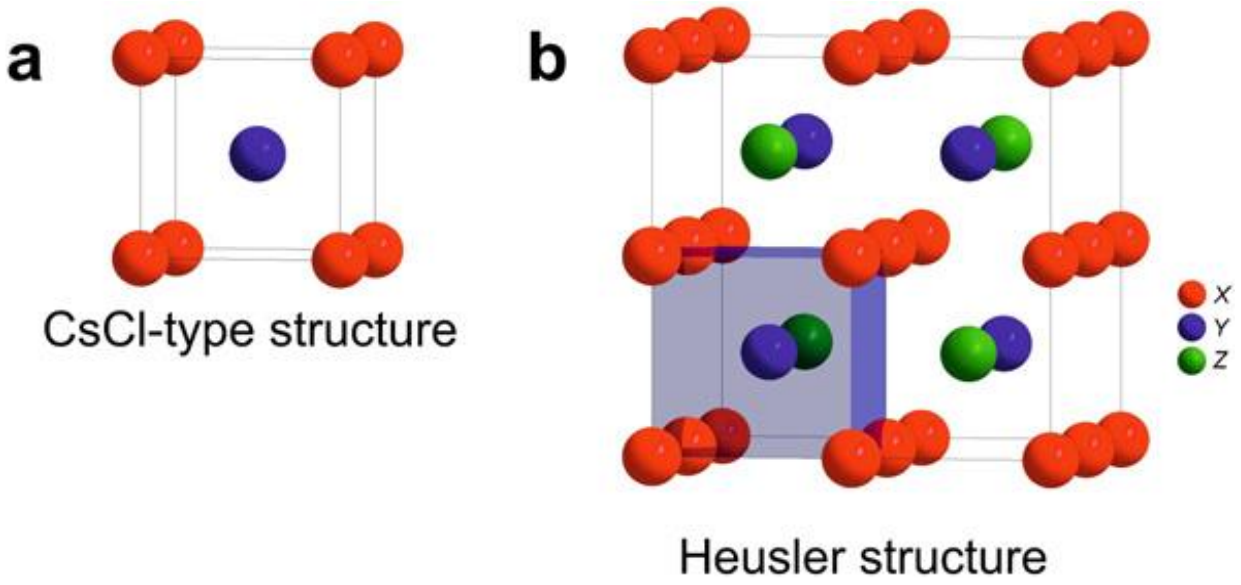

Figure I.3: *(a) CsCl structure and (b) the Heusler structure which is shifted by (1/4, 1/4, 1/4) with respect to the standard cell to make the CsCl superstructure visible.*

In addition to the structure described above, an inverse Heusler structure is observed Instead, they are placed on the Wyckoff positions 4a (0, 0, 0) and 4d (3/4, 3/4, 3/4), while the Y and the Z atoms are located at 4b (1/2, 1/2, 1/2) and 4c (1/4, 1/4, 1/4), respectively. The prototype of this structure is $AgLi_2Sb$ with space group F43m (Space group no. 216) [21].

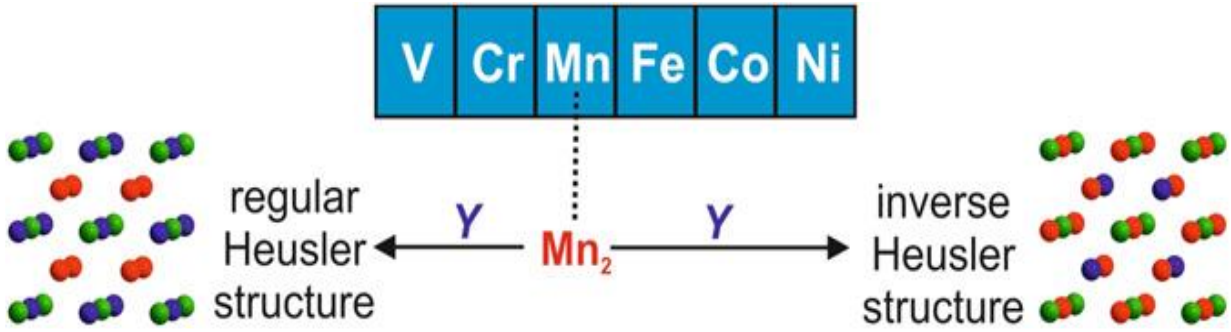

Figure I.4: *Mn_2-based Heusler compounds form both, the inverse and the regular structure, depending on the element on the Y position.*

This structure calculation show that already small amounts of disorder within the distribution of the atoms on the lattice sites cause distinct changes in their electronic structure, and thus also in their properties. Therefore, a careful analysis of their crystal structure is essential to understand the structure-to-property relation of Heusler compounds [22].

I.3.2.2.Order-disorder phenomena for Heusler structure:

Similar to the Half-Heusler materials, the properties of Heusler compounds are strongly dependent on the atomic order. The different ordering variants of Heusler compounds are summarizes in **Table.I.3**.

TableI.3: Site occupancy and general formula for different atomic order of Heusler compounds. The notations according to the Inorganic Crystal Structure Database (ICSD), the Strukturberichte (SB), the Pearson database, as well the space group are given [23].

Site occupancy	General formula	Structure type ICSD	Structure type SB	Structure type Pearson	Space group
X, X', Y, Z	XX'YZ	LiMgPdSn	Y	cF16	F43m(No. 216)
X =X, Y,Z	X_2YZ	Cu_2MnAl	$L2_1$	cF16	Fm3m(No. 225)
X, X' = Y,Z	$XX_2'Z$	$CuHg_2Ti$	X	cF16	F43m(No. 216)
X =X' = Y,Z	X_3Z	BiF_3	DO_3	cF16	Fm3m(No. 225)
X =X' , Y=Z	X_2Y_2	CsCl	B2	cP2	Pm3m(No. 221)
X =Y, X' =Z	X_2X_2'	NaTl	B32	cF16	Fd3m(No. 227)
X =X'= Y=Z	X_4	W	A2	cI2	Im3m(No. 229)

I.3.3.Qaternary compounds:

Quaternary Heusler compounds with the 1:1:1:1 stochiometry have the general formula XX'YZ. There are two different elements X and X'. They are located at the 4a (0, 0, 0), and 4d (1/4, 1/4, 1/4). positions, respectively, Y is placed on 4b (1/2, 1/2, 1/2), and Z on 4c (3/4, 3/4, 3/4), Where the valence of X' is lower than the valence of X atoms and the valence of the Y element is lower than the valence of both X and X'. The sequence of the atoms along the fcc cube's diagonal is X-Y-X'-Z which is energetically the most stable [24]. This structure has the

prototype LiMgPdSn [10] and crystallizes in (space group no. 216, F43m). An illustration of the inverse Heusler structure and the quaternary variant is given in Figure.I.5

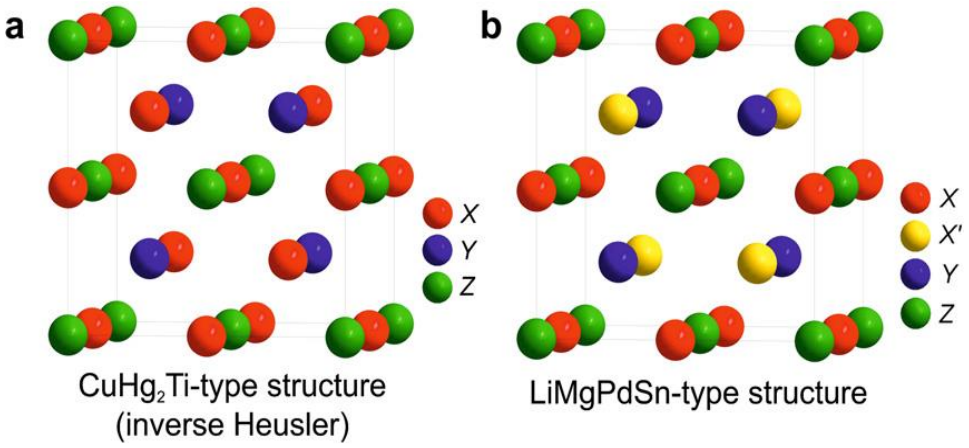

Figure I.5: *(a) The inverse Heusler structure $CuHg_2Ti$ and (b) the quaternary version LiMgPdSn.*

I.4 Heusler compounds electronic classification:

Heusler compounds can be ferromagnetic, Half-metallic, and semiconductor according to their electronic behavior.

I.4.1.Ferromagnetic Heusler compounds:

Heusler compounds first attracted interest among the scientific community in 1903 when Fritz Heusler discovered that an alloy with the composition Cu2MnAl behaves like a ferromagnet, although non of its constituent elements is magnetic by itself [17, 18].This remarkable material and its relatives, which by now comprise a vast collection of more than 1000 compounds, are now known as Heusler compounds. They are ternary semiconducting or metallic materials with a 1:1:1 (also known as “Half-Heusler”) or a 2:1:1 (Full Heusler) stoichiometry. Surprisingly, the properties of many Heusler compounds can be predicted by simply counting the number of valence electrons [25].Recently, they attracted great interest due to their potential application in spintronics and the green energy-related fields, such as solar cells or thermoelectric (TEs).

I.4.2.Half-metalic Heusler compounds:

The large family of magneto-electrical Heusler compounds, the half-metallic ferromagnets are semiconducting for electrons of one spin orientation, whereas they are metallic for electrons with the opposite spin orientation. Such compounds exhibit nearly full spin polarized conduction electrons, making them suitable materials for spintronic applications. Heusler compounds continuously attract interest duo to their high Curie temperatures [26] and, in fact, are being used today in magnetic tunnel junctions [27].

I.4.3.Semi-conductors Heusler compounds:

Heusler compounds with eight valence electrons incorporate an impressive group of unconventional semiconductors. Ternary semiconductors are closely related to silicon and binary semiconductors such as GaAs. However, the design of unconventional semiconductors based on 18 for half-Heusler compounds or 24 valence electrons for Heusler compounds is also possible, resulting in band gap widths of more than 1 eV. Indeed, the remarkable properties have been demonstrated recently.

In the next chapter we will give more detail for Half-Heusler semiconductors properties.

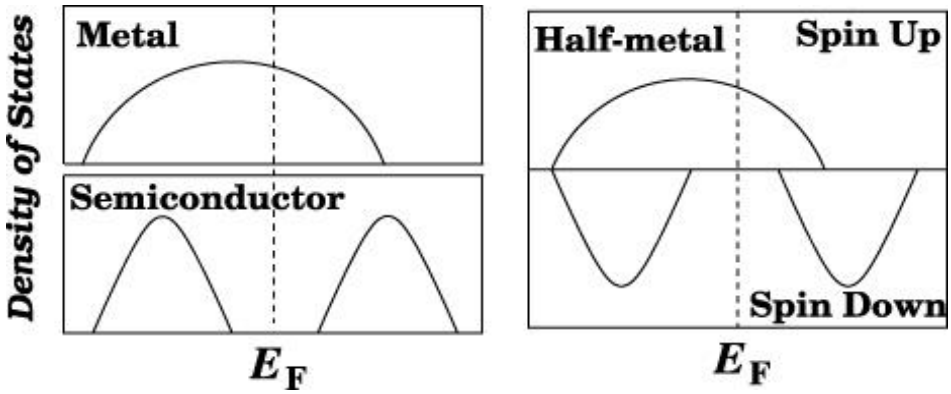

Figure I.6.*Shematic representation of density of states for: Metals, Half-metals, and Semiconductors* [28]**.**

I.5.Heusler compounds Applications:

The world at present is facing major problems such as energy crisis and environmental impact. Thermoelectricity is considered to be one of the potential ways towards addressing both these problems. However Half-Heusler materials having semiconducting [29, 30] properties are considered to be potential thermoelectric materials because of their large temperature stability. Furthermore, these materials are easy to synthesize and more environmental friendly since they consist of non-toxic elements.

I.6.Conclusion:

This chapter gives a broad overview of an outstanding class of materials, the Heusler compounds. Summarize all important aspects concerning these exceptional materials. Crystal structure and order-disorder phenomenon in relation to multifunctional tunable properties were discussed. Many fascinating research projects will certainly emerge in future which take advantage of their tunable functionalities. Heusler compounds having semiconducting properties based devices could be designed according to the specific needs of the corresponding application and the new, unknown multifunctional properties could be developed with plenty of technological applications in thermoelectric. All within the one material class, the Heusler compounds.

Bibliography:

1. Tuzcuoglu, H., *Corrélation entre les propriétés structurales et magnétiques des couches minces et nanostructures de Co_2FeAl*, 2014.
2. Mouche, L., M. Meuris, and M. Heyns, *Light point defect generation during photoresist spin coating: Characterization and controlling parameters.* Journal of the Electrochemical Society, 1997. **144**(10): p. 3608.
3. ZENASNI, H., *Etude théorique des propriétés Magnétiques, électroniques et structurales des alliages Heusler*, 2013.
4. Sakurada, S. and N. Shutoh, *Effect of Ti substitution on the thermoelectric properties of (Zr, Hf) NiSn half-Heusler compounds.* Applied physics letters, 2005. **86**(8): p. 082105.
5. Schuster, H., et al., *Investigations on neutron diffraction of the phases LiAlSi and LiAlGe.* Z. Naturforsch., B, 1976. **31**(11): p. 1540-1541.
6. Hohl, H., et al., *Efficient dopants for ZrNiSn-based thermoelectric materials.* Journal of Physics: Condensed Matter, 1999. **11**(7): p. 1697.
7. Sebastian, C.P., et al., *Crystal chemistry and spectroscopic properties of ScAuSn, YAuSn, and LuAuSn.* Solid state sciences, 2006. **8**(5): p. 560-566.
8. Ritchie, L., et al., *Magnetic, structural, and transport properties of the Heusler alloys Co 2 MnSi and NiMnSb.* Physical Review B, 2003. **68**(10): p. 104430.
9. Morcrette, M., et al., *Influence of electrode microstructure on the reactivity of Cu2Sb with lithium.* Electrochimica acta, 2007. **52**(17): p. 5339-5345.
10. Dai, X., et al., *New quarternary half metallic material CoFeMnSi.* Journal of applied physics, 2009. **105**(7): p. 07E901.
11. Miura, Y., K. Nagao, and M. Shirai, *Atomic disorder effects on half-metallicity of the full-Heusler alloys Co 2 (Cr 1− x Fe x) Al: A first-principles study.* Physical Review B, 2004. **69**(14): p. 144413.
12. Pishtshev, A., E. Strugovshchikov, and S. Karazhanov, *Theoretical design of yttrium oxyhydrides: Remarkable richness of phase diagram.* 2018.
13. Villars, P., *Calvert LD Pearson's handbook of crystallographic data for intermetallic phases.* ASM International, Ohio, 1991. **3**: p. 2465-2466.
14. Nuss, J. and M. Jansen, *Zur Abgrenzung der PbFCl-und Cu2Sb-Strukturfamilien: Neubestimmung und Verfeinerung der Kristallstrukturen von CuMgSb, Cu2Sb und CuMgAs.* Zeitschrift für anorganische und allgemeine Chemie, 2002. **628**(5): p. 1152-1157.
15. Skovsen, I., et al., *Multi-temperature synchrotron PXRD and physical properties study of half-Heusler TiCoSb.* Dalton transactions, 2010. **39**(42): p. 10154-10159.
16. Bacon, G. and J. Plant, *Chemical ordering in Heusler alloys with the general formula A2BC or ABC.* Journal of Physics F: Metal Physics, 1971. **1**(4): p. 524.
17. Mokhtari, M., et al., *Ab Initio Investigation of Structural Stability and Electronic and Magnetic Properties of the Half-Heusler Alloys: MTiSb (M= Fe, Co, and Ni).* Journal of Superconductivity and Novel Magnetism, 2018. **31**(9): p. 2991-2998.
18. Heusler, F., *Mangan-aluminium-kupferlegierungen.* Verh. DPG, 1903. **5**: p. 219.
19. Heusler, O., *Crystal structure and the iron magnetism of manganese-aluminium-copper alloys.* Ann. Phys, 1934. **19**: p. 155-201.
20. Bradley, A.J. and J. Rodgers, *The crystal structure of the Heusler alloys.* Proceedings of the royal society of london. Series A, Containing Papers of a Mathematical and Physical Character, 1934. **144**(852): p. 340-359.
21. Kandpal, H.C., C. Felser, and R. Seshadri, *Covalent bonding and the nature of band gaps in some half-Heusler compounds.* Journal of Physics D: Applied Physics, 2006. **39**(5): p. 776.
22. Webster, P.J., *Heusler alloys.* Contemporary Physics, 1969. **10**(6): p. 559-577.
23. Graf, T., et al., *Crystal structure of new Heusler compounds.* Zeitschrift für anorganische und allgemeine Chemie, 2009. **635**(6-7): p. 976-981.
24. Alijani, V., et al., *Quaternary half-metallic Heusler ferromagnets for spintronics applications.* Physical Review B, 2011. **83**(18): p. 184428.
25. Felser, C., G.H. Fecher, and B. Balke, *Spintronics: a challenge for materials science and solid-state chemistry.* Angewandte Chemie International Edition, 2007. **46**(5): p. 668-699.
26. Wurmehl, S., et al., *Investigation of Co 2 Fe Si: The Heusler compound with highest Curie temperature and magnetic moment.* Applied physics letters, 2006. **88**(3): p. 032503.
27. Wang, W., et al., *Coherent tunneling and giant tunneling magnetoresistance in Co 2 FeAl/MgO/CoFe magnetic tunneling junctions.* Physical Review B, 2010. **81**(14): p. 140402.
28. Galanakis, I. and P.H. Dederichs, *Half-metallic alloys: fundamentals and applications.* Vol. 676. 2005: Springer.

29. Crooker, S., et al., *Terahertz spin precession and coherent transfer of angular momenta in magnetic quantum wells.* Physical review letters, 1996. **77**(13): p. 2814.
30. Araki, S., et al., *Which spin valve for next giant magnetoresistance head generation?* Journal of applied physics, 2000. **87**(9): p. 5377-5382.

Chapter II

Results and Discussions

II.1. Introduction:

The search of new semiconducting compounds for thermoelectric and photovoltaic applications becomes necessary. Therefore, filled tetrahedral compounds have been studied extensively [1-8]. Zunger et al. [1, 2, 4] have predicted the bang gap nature, by inserting of small atoms at tetrahedral interstitial states, of zinc blende semiconductors. Nowotny–Juza compounds of the form $A^{I}B^{II}C^{V}$ were predicted to be a new group of direct gap semiconductors [1, 2] in the range of 1.3–2 eV. So these compounds are predicted to be promising candidates for optoelectronics and anode materials for Lithium batteries. In order to

discover new interesting materials for thermoelectric applications, the electronic structure of LiZnSb was analyzed in detail and has been suggested as a potential new thermoelectric material [8].

LiZnN is considered to be one of filled tetrahedral $A^{I}B^{II}C^{V}$ compounds [1, 2, 9-13] having a structure of a $B^{II}C^{V}$ zinc blende lattice with A^{I} atoms filling half of the available tetrahedral interstitial sites. This structure has been focused on because of its similarity to III-V semiconductors with small atoms filling tetrahedral interstitial sites in the viewpoint of the band structure modification. The structure of LiZnN is shown in figure.II.1.

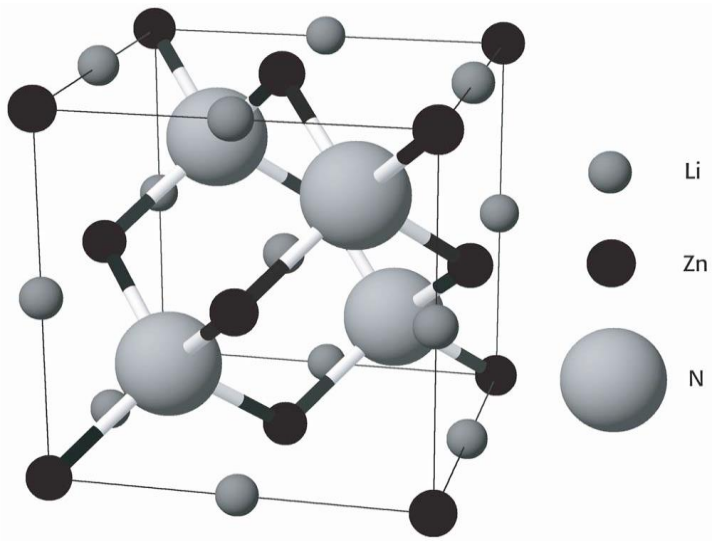

Figure.II.1. *Crystal structure of LiZnN.*

II.2.Calculations details:

The calculations presented in this work were performed within the Density functional theory (DFT)[14] and the full potential linearized augmented plane wave (FP-LAPW) method. We use the WIEN2k [15] implementation of the method which allows the inclusion of local orbital in the basis, improving upon linearization and making possible a consistent treatment of the semi core and valence states in an energy window, hence ensuring proper orthogonality. The electron–electron interaction was treated within generalized gradient approximation (GGA) by Perdew, Burke and Ernzerhof (PBE) exchange–correlation potential[16]. In this method the space is divided into non-overlapping muffin-tin (MT) spheres separated by an interstitial region, in this context the basis functions are expanded in combinations of spherical harmonic functions inside the muffin-tin spheres and Fourier series in the interstitial region. The muffin-tin sphere radii (R_{MT}) are showed in **table II.1**.

The basis functions are expanded up to R_{MT}*Kmax = 8 (where Kmax is the plane wave cut-off and R_{MT} the smallest of all MT sphere radii) and for the integration we used 30× 30 × 30 k-points mesh in the whole first Brillouin zone.

Table.II.1: R_{MT} value for the different atoms Li, Zn, and N.

Atoms	**Li**	**Zn**	**N**
R_{MT}	**1.72**	**2.04**	**1.67**

Table.II.2: Electronic configuration for the different atoms Li, Zn, and N.

Atoms	**Li**	**Zn**	**N**
Electronic configuration	**2S1**	**4S2 3d10**	**$2S^2$ 2P3**

II.3. structural Properties:

The structural properties are the main step in investigating the behavior of some material. In our work the structural properties were calculated using GGA for the non-magnetic (NM), and ferromagnetic (FM) states. These calculations for the half- Heusler: LiZnN.

The space group of our studied compounds LiZnN is F43m (space gr. No. 216). LiZnN can have three different structure type as **table**.**II.3** shows.

Table II.3: The Wyckoff positions for the atoms: Li, Zn, and N.

	4a(0,0,0)	4b(1/2,1/2,1/2)	4c(1/4,1/4,1/4)
Type I	**Li**	**Zn**	**N**
Type II	**N**	**Li**	**Zn**
Type III	**Zn**	**N**	**Li**

II.3.1.total energies and mesh parameter:

The structures of all compounds were optimized by calculating the total energy as a function of volume, which was followed by fitting the results with Birch Murnaghan [17]equation of state:

$$E_{tot}(V) = E_0(V) + \frac{9\,B_0V}{16}\left[B'\left\{\left(\frac{V_0}{V}\right)^{2/3} - 1\right\}^3 + \left\{\left(\frac{V_0}{V}\right)^{2/3} - 1\right\}^2\left\{6 - 4\left(\frac{V_0}{V}\right)^{2/3}\right\}\right] \qquad \text{II-1}$$

Where:

- E (V) represents the total energy as a function of the unit cell volume.
- V_0 is the cell volume at ambient conditions.
- V is the deformed volume.
- B_0 is the bulk modulus.
- B_0' is the derivative of the bulk modulus.

The bulk modulus and its derivative are usually obtained from fits to experimental data and are defined as:

$$B = V \frac{\partial^2 E}{\partial V^2} \qquad \text{II-2}$$

The calculated energy curves in function of volume for LiZnN are displayed in **figure.II.2.**

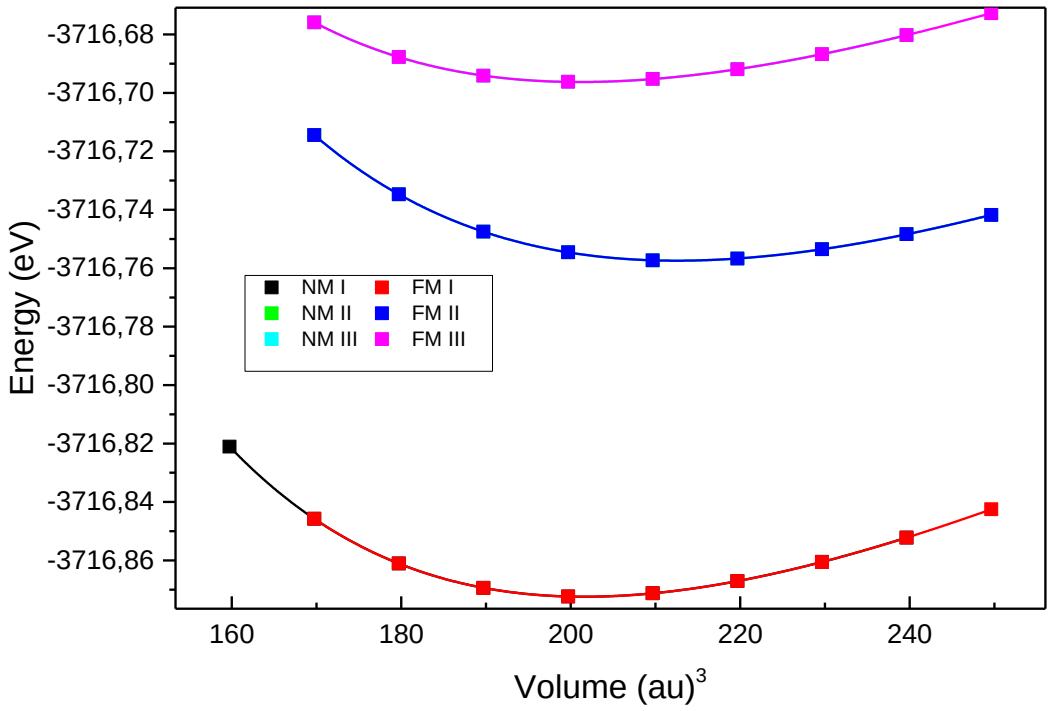

Figure II.2: *Variation of total energy as a function of volume for LiZnN.*

The figure shows that our compound is more stable in the phase NM type I which correspond to the lowest energy.

The results of structural optimization of LiZnN are listed in table.II.4 with the available experimental data and results of other calculations.

Table II.4: Calculated lattice parameter (a), bulk modulus (B) and its derivative (B'), unit cell volume (V_0), total energy (E_0).

	Type	a (Bohr)	V_0	B (GPA)	B'(GPA)	E_0 (Ry)
Our Calculations	**NM I**	**4.9257**	**201.6287**	**113.7447**	**4.4615**	**-3716.872416**
	FM I	4.9257	201.6204	113.7404	4.4853	-3716.872426
	NM II	5.0129	212.5223	96.2544	4.6350	-3716.757421
	FM II	5.0129	212.5242	96.2514	4.6345	-3716.757419
	NM III	4.9217	201.1361	88.9727	4.6543	-3716.696275
	FM III	4.9217	201.1322	88.9892	4.6568	-3716.696275
Experimental		4.91[6]				
Other Calculations		4.80[18]		141[18]		
		4.7669 [19]		145[19]		

From reported values in the above table, it's clear that, our calculated values are close to the theoretical and experimental results.

II.4. Elastic Properties:

II.4.1.Introduction:

Now we turn our attention to study the elastic properties of our compound via calculating the elastic constant C_{ij} C_{11}, C_{12}, C_{13}, C_{33}, C_{44} and C_{66} using the FP-LAPW method . A cubic crystal has only three independent elastic constants; C_{11}, C_{12}, C_{44}.

The elastic constants C_{ij} denote the stability and stiffness (rigidity) of the compounds which are determined by calculating the total energy as a function of strain by using the Mehl method[20]. For the calculation of the modulus $C_{11} - C_{12}$ I used the volume-conserving orthorhombic strain tensor:

$$\bar{\epsilon} = \begin{bmatrix} \delta & 0 & 0 \\ 0 & -\delta & 0 \\ 0 & 0 & \frac{\delta^2}{(1-\delta^2)} \end{bmatrix} \qquad \text{II-3}$$

Application of this strain changes the total energy from its unstrained value to:

$$E(\delta) = E(-\delta) = E(0) + (C_{11} - C_{12})V_0\,\delta^2 + O(\delta^4) \qquad \text{II-4}$$

Where:

- V is the volume of the unit cell.
- E (0) is the energy of the unstrained lattice at volume V.

For the elastic modulus C_{44}, we used the volume-conserving monoclinic strain tensor:

$$\vec{\epsilon} = \begin{bmatrix} 0 & \frac{\delta}{2} & 0 \\ \frac{\delta}{2} & 0 & 0 \\ 0 & 0 & \frac{4}{(4-\delta^2)} \end{bmatrix} \qquad \text{II-5}$$

The total energy changes this time to:

$$E(\delta) = E(-\delta) = E(0) + \frac{1}{2}C_{44}V_0\delta^2 + O(\delta^4) \qquad \text{II-6}$$

For isotropic cubic crystal, the bulk modulus B shows the resistance to fracture[21]. It has been calculated by the given expression:

$$B = \frac{C_{11}+2C_{12}}{3} \qquad \text{II-7}$$

The values of Poission ratio (ν), Zener anisotropy factor (A), Bulk modulus (B), Shear modulus (G), and Young modulus (E), have been calculated using the following relations: The reported results are listed in **Table.II.5**.

$$\mathrm{G} = \frac{1}{5}(3\mathrm{C44} + \mathrm{C11} - \mathrm{C12}) \qquad \text{II-8}$$

$$A = \frac{2C_{44}}{C_{11}-C_{12}} \qquad \text{II-9}$$

$$E = \frac{9BG}{3B+G} \qquad \text{II-10}$$

$$\nu = \frac{1}{2}\left(1 - \frac{E}{3B}\right) \qquad \text{II-11}$$

The cubic structure of our compound will be mechanically stable if it satisfies the stability criteria of Born–Huang given by:

$(C_{11} - C_{12}) > 0$, $C_{11} > 0$, $C_{44} > 0$, $C_{11} > C_{12}$, $(C_{11} + 2C_{12}) > 0$ and $C_{12} < B < C_{11}$. According to Table.II.4 results the born criteria are realized which confirms the stability of our compound LiZnN. The shear modulus G represents plastic deformation[21] equal to 87.64 GPa .Young's modulus named after the British scientist Thomas Young [22] estimates the stiffness of a solid material equal to 211.15 GPa . Poisson's ratio ν named after the French Siméon Poisson describes the contraction of a material in directions perpendicular to the direction of loading equal to 0.20 which is lower than 0,25 that indicates the non-centralization of the inter forces of our material , since $0.25 < \nu < 0.50$ [23].

The elastic coefficients are also related to the ductile or brittle properties of the metals by the empirical relation (B/G)[24, 25] .where B is the bulk modulus and G is the shear modulus as we mentioned. Frantsevich et al.[26] have suggested that if B/G > 1.75, the material has ductile nature, otherwise behaves in a brittle way. In the present calculation, the value of B/G has been found to be 1.35, which shows that our compound is brittle in nature; the value of B/G is always greater than one, which suggests that volume compression is more than shear compression.

The Zener anisotropy factor (A) named after Clarence Zener [27] is a dimensionless number that is used to quantify the anisotropy for a cubic crystal. Where the value of one means that the material is isotropic. While any other value greater or less than one indication the anisotropy characteristic. The Zener anisotropy factor (A) has been calculated and found to be 0.60. This shows that our semiconductor LiZnN is an anisotropic material.

Table II.5: The values of Poisson's ratio (ν), Zener anisotropy factor (A), Bulk modulus B (GPa), shear modulus G (GPa) and Young modulus E (GPa), elastic constants C_{ij} (GPa).

C_{11}	C_{12}	C_{44}	B	E	G	ν	B/G	A
277.31	**40.11**	**71.45**	**119.17**	**211.15**	**87.64**	**0.20**	**1.35**	**0.60**

II.4.2.Debye temperature :

Debye temperature is obtained from elastic data using the average wave velocity and mean atomic volume which corresponds to the upper limit of phonon frequency in a crystal lattice and calculated using the following relation:

$$\theta_D = \frac{h}{k}\left[\frac{3n}{4\pi}\left(\frac{N_A\rho}{M}\right)\right]^{\frac{1}{3}} v_m \qquad \text{II-12}$$

Where

- *h is* Plank constant.
- *k Boltzamann* constant.
- *Na* Avogadro number.
- *n* number of atoms in a molecul.
- *M* the molecular weight.
- ρ The density .
- v_m The average wave velocity.

.

v_m is the average wave velocity and is dependent to transverse v_t and longitudinal v_l wave velocity due to following formulas:

$$v_m = \left[\frac{1}{3}\left(\frac{2}{v_t^3} + \frac{1}{v_l^3}\right)\right]^{\frac{1}{3}} \qquad \text{II-13}$$

Where:

$$v_l = \sqrt{\frac{3B+4G}{3\rho}} \qquad \text{II-14}$$

$$v_t = v\sqrt{\frac{G}{\rho}} \qquad \text{II-15}$$

Debye temperature and the melting temperature have been computed and found to be equal to 652.15K and 2191.90+300K respectively (see Table.II.6).

Table.II.6: Presents the average, transverse, and the longitudinal (v_m ,v_t ,v_l) wave velocity respectively in m/s, Debye temperature $\boldsymbol{\Theta_D}$ in K, and the melting temperature in K.

v_m	v_l	v_t	Θ_D	T_m
4697.78	6979.84	4283.15	652.15	2191.90+300

II.5.Electronic properties:

In order to discuss the electronic structure in detail, we have calculated the band structures, total density of states (DOS) and partial density of states (DOS) of LiZnN.

II.5.1.band structure:

The band structure of a solid describes those ranges of energy, called energy bands, that an electron within the solid may have (“allowed bands”) and ranges of energy called band gaps (“forbidden bands”), which it may not have. Band theory models the behavior of electrons in solids by applying the existence of energy bands. This theory successfully uses a material’s band structure to explain many physical properties of solids. Bands may also be viewed as the large-scale limit of molecular orbital theory. The Fermi level $\boldsymbol{E_F}$ is set at 0 eV (dotted horizontal line). By definition, the difference between the maximum of the valence band and the minimum of the conduction band is the fundamental energy gap for insulators materials and semiconductor[28].

Using FP-LAPW method witing GGA approximation we have calculated band structure and density of states of our compound LiZnN witch shows that the top of valence band and the bottom of the conduction band are all at the Γ symmetry point, which indicate that our compound is a semiconductor direct gap material, having band gap energy value E_g =0.519 eV. The band structure calculations have been shown in **Figure II.3.**

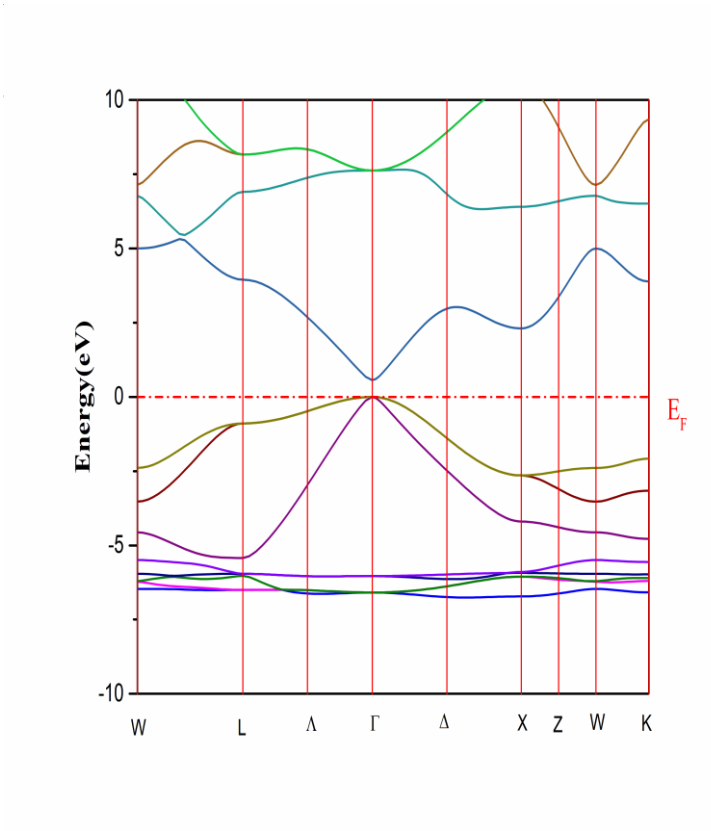

Figure II.3: *Band structure for LiZnN.*

II.5.2.Density of states:

In solid state physics and condensed matter physics, the density of states (DOS) is a fundamental quantity in band theory which describes the number of states that are to be occupied by the system at each level of energy.

The partial density of states (PDOS) and total density of states (TDOS) plays vital role to explain the physical properties of semiconductor compounds.

Figure.II.4 represents the total and partial Density of states (States/eV) of LiZnN obtained within GGA approximation, and were investigated in the energy range from -10 to 14.2.

- The valence band region of LiZnN lies between -6.79 eV to Fermi energy level (EF) and divided into two sets: low and high-energy sets of bands. The low-energy set extending from -6.79 eV to -5.53 eV is dominantly formed by Zn-d states. The higher-energy set of valence band ranging from -5.53 eV to Fermi energy level is mainly due to Li-s and N- p states with a negligible contribution of Zn-s and N-s states.
- The conduction band region consists mainly of Li-s and N-s/p states in the energy range from 5 to 10 eV.
- We also find that our compound has a direct gap with a forbidden band gap of $E_g = 0.519$. This result confirms the semiconducting behavior of LiZnN.

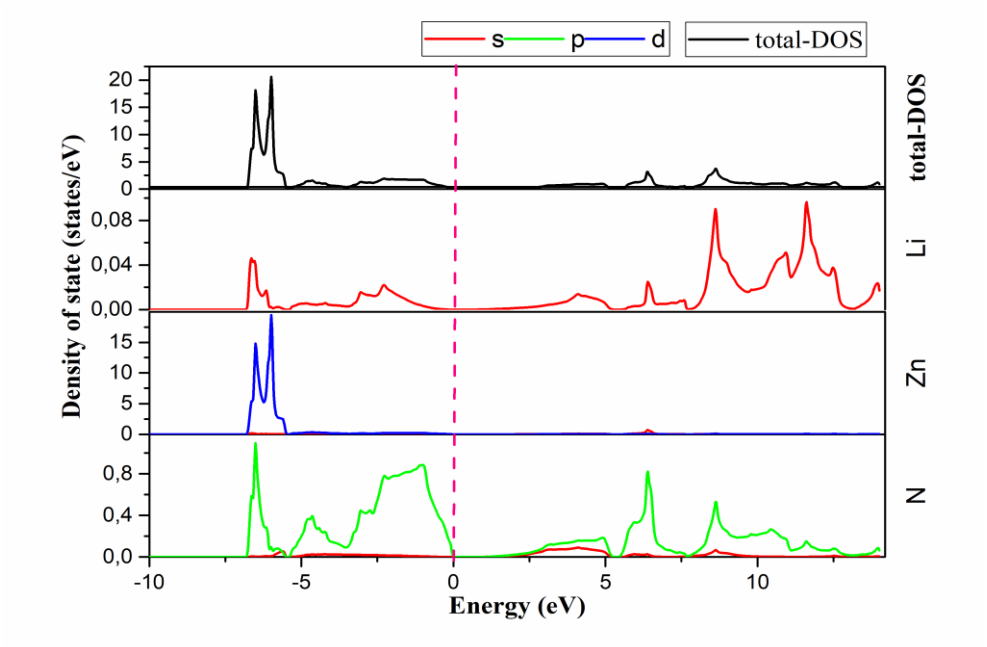

Figure II.4: *The total and partial Density of states (States/eV) of LiZnN.*

II.6.Optical properties:

II.6.1.Introduction:

In solid state physics, it is of great interest to know the different ways in which light interacts with matter, such as absorption, transmission, reflection, scattering, and emission. First, we will present the dielectric function within the framework of quantum mechanics, and then we will determine the link between the real and imaginary part of the dielectric function and the complex index through the Kramers-Kronig relations.

II.6.2.Dielectrique function:

Optical properties can be obtained from the dielectric function. The dielectric function,

$$\varepsilon(\omega) = \varepsilon_1(\omega) + i\varepsilon_2(\omega) \qquad \text{II-16}$$

ε_1 represents the real part while ε_2 represents the imaginary part, In reality, the imaginary part $\varepsilon_2(\omega)$ is calculated from the joint density of states ≪ Joint Density of States ≫ (JDOS). The real part $\varepsilon_1(\omega)$ is deduced from $\varepsilon_2(\omega)$ by using the Kramer-Kronig, it is relations are these two quantities which provide the set of electrical and optical characteristics of a material.

The imaginary part:

Figure II.5 illustrates the imaginary part of the dielectric function of the LiZnN material in the energy range from 0 eV to - 13 eV. In this figure II.5, we notice that $\varepsilon_2(\omega)$, presents an increase from 0.53 eV which is the first occurrence denoted E_0. It designates direct optical transitions. The first main peak is located at around 1.48 eV, the second at 5.23 eV, while the others are located at values of 7.76, 8.25 and 9.42 eV respectively. This is shown in Table.II.7.

Table.II.7. Diffrentes peaks in (eV) of the imaginary part $\varepsilon_2(\omega)$ as well as the dielectric constant $\varepsilon_1(\omega)$ and the refractive index n (ω).

LiZnN	E_0	E_1	E_2	E_3	E_4	E_5	$\varepsilon_1(0)$	n(0)
	0.53	**1.48**	**5.23**	**7.76**	**8.25**	**9.42**	**6,95**	**2,6**

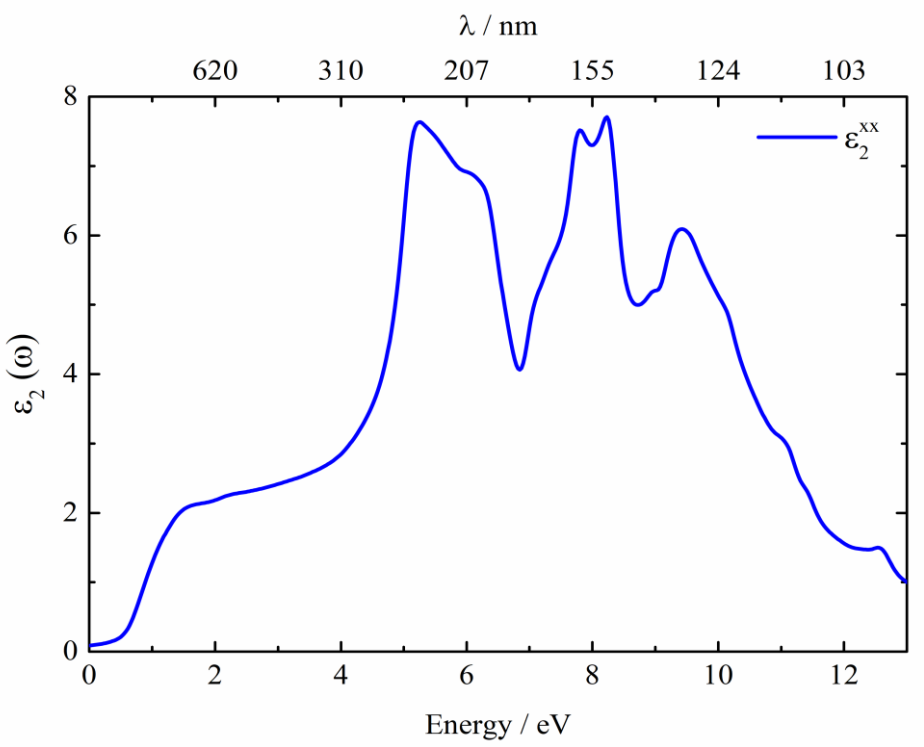

Figure II.5: *The imaginary part of the dielectric function curves for LiZnN.*

The maximum absorption for the compound is located at 7.70 eV, the imaginary part of the dielectric function shows a main peak in the UV region and almost all other peaks are in the UV region.

The real part:

The figure II.6, shows that, the real part $\varepsilon_1(\omega)$ increases according to the energy of the photons, to reach a peak for an energy equal to 0.85. Then it decreases in the spectral part of the visible, then increases again in the UV regions reach a maximum for an energy value equal to 4.94 eV, after the limit of the maximum value of the function $\varepsilon_1(\omega)$, the spectrum decreases with small oscillations at higher energies, ranging from 6eV to 13 eV, The real part, $\varepsilon_1(\omega)$ of the static dielectric function at 0eV for LiZnN is equal to 6.95. The passage through the zero value of the spectrum means that there is no scattering. It should be noted that at this energy value, the dispersion is zero, and therefore the absorption is maximum.

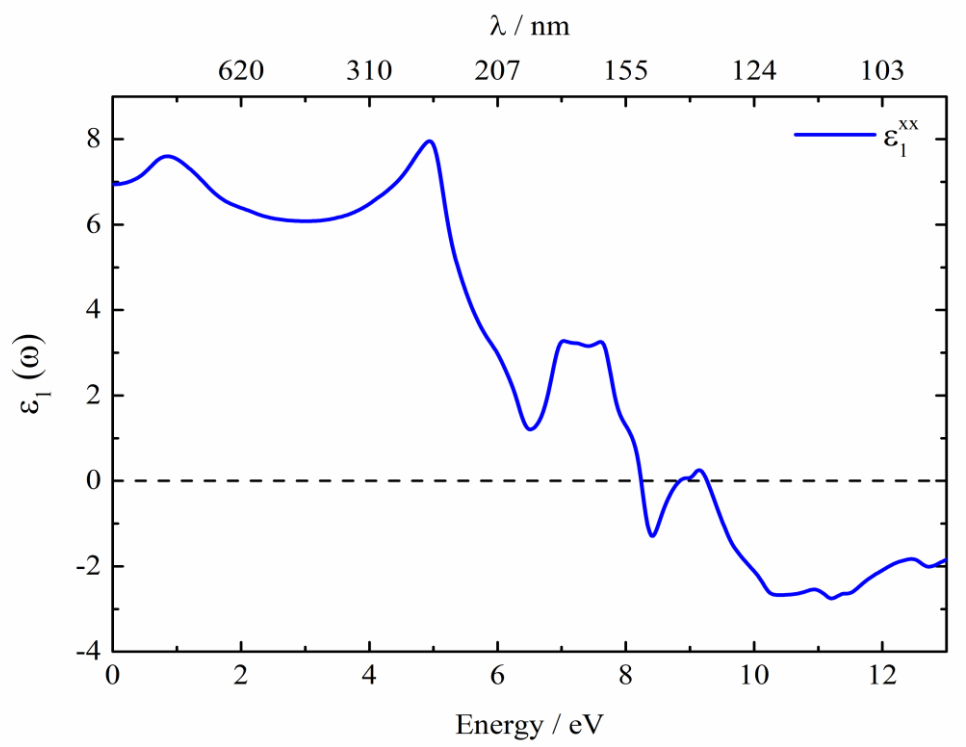

Figure II.6: *The real part of the dielectric function curves for LiZnN.*

II.6.3.Absorption coefficient:

Using the real and imaginary parts of dielectric function, the optical absorption coefficient defined as:

$$\alpha(\omega) = \frac{4\pi k(\omega)}{\lambda} \qquad \text{II-17}$$

Where k (ω) is the extinction coefficient and λ represents the wavelength of light in vacuum. The absorption of photons is at the origin of the interband optical transition. The evolution of the absorption coefficient is shown in Figure II.7. From this figure, we can see that absorption starts from 0.53eV energy.

The fundamental absorption threshold starts at approximately 0.53eV this value corresponds to the energy gap for LiZnN. Figure (II.7) shows that the absorption starts to increase constantly from the value 0.53 eV which corresponds to the IR spectral region, up to the energy value 13 eV which corresponds to the far UV spectral region. It can also be seen that this material is very useful for optoelectronic devices operating in the ultraviolet range.

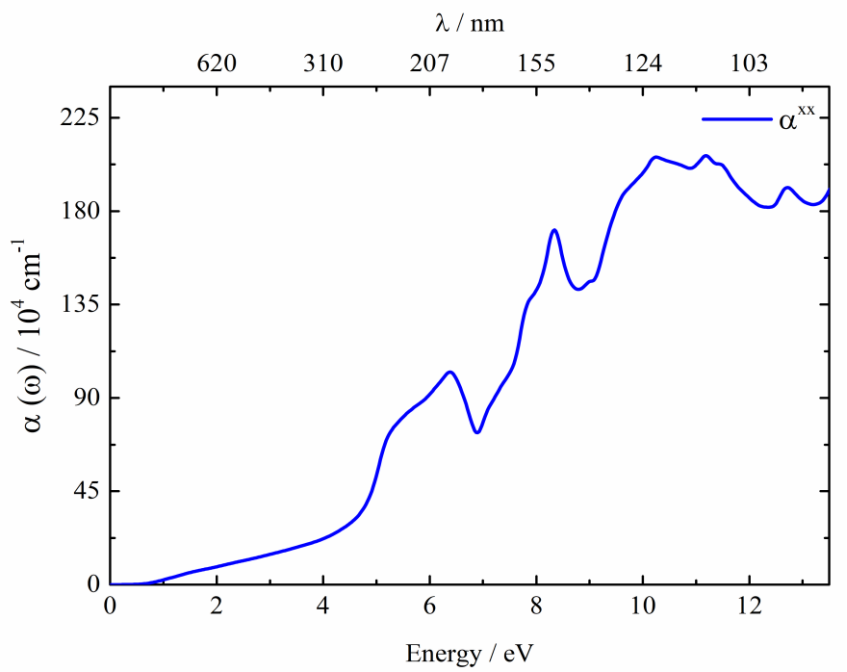

Figure II.7: *The absorption coefficient for LiZnN.*

II.6.4.Reflictivity spectrum:

Another very important parameter is the reflectivity coefficient *R* that characterizes the reflective energy part of the interface of the solid and can be deduced by the refraction index. Reflectivity index depends on incident photon energy. Main peaks in the reflectivity spectrum are corresponding to interband transitions [29]. The reflectivity can be calculated by equation:

$$R(\omega) = \left|\frac{\tilde{n} - 1}{\tilde{n} + 1}\right| = (n - 1)^2 + \frac{k^2}{(n + 1)^2} + k^2 \qquad \text{II-18}$$

Where:

- N: is the complex refractive index.
- n : is the refractive index.
- k : is the extinction coefficient.

Figure II.8.shows that the reflectivity starts to increase constantly from the value R (0) =.20 eV which corresponds to the IR spectral region, up to the energy value 13 eV which corresponds to the far UV spectral region.

The behavior of the reflectivity spectra, R (ω) of our alloy is plotted in this graph shows a variable pattern at range energy from 0eV to 13eV.

Table.II.8: shows the reflectivity main peak within its width**.**

LiZnN	
Peak	**13**
Width	**13**

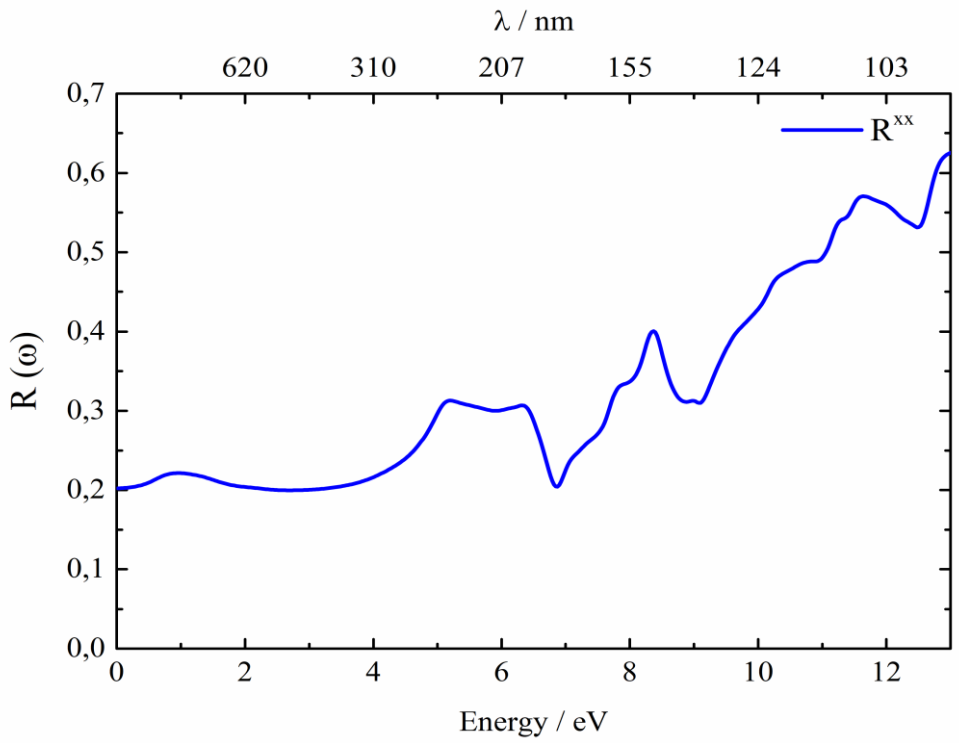

Figure II.8: *The reflectivity for LiZnN.*

II.6.4.Refrative index:

For optical materials, the knowledge of the refractive index n (ω) is essential for its use as photonic and optical devices, waveguides, solar cells and detectors. The refractive index n (ω) is related to microscopic atomic interactions and it is a very important physical parameter [30-37], we consider the crystal as a collection of electric charges. On the other hand, the refractive index will be related to the density and local polarizability of these entities [29, 38].

$$n(\omega) = \left(\frac{\varepsilon_1(\omega) + \sqrt{+\varepsilon_1^2(\omega) + \varepsilon_2^2(\omega)}}{2} \right)^{1/2} \qquad \text{II-19}$$

The refractive index of the semiconductor n (ω) is calculated from the real part of the dielectric function:

$$n(\boldsymbol{\omega}) = \sqrt{\varepsilon_1(\omega)} \qquad \text{II-20}$$

Figure II.9 shows the variation of the refractive index n (ω) of the LiZnN compound as a function of the incident photon energy. The refractive index at 0eV for LiZnN is equal to n (0) = 2.64.

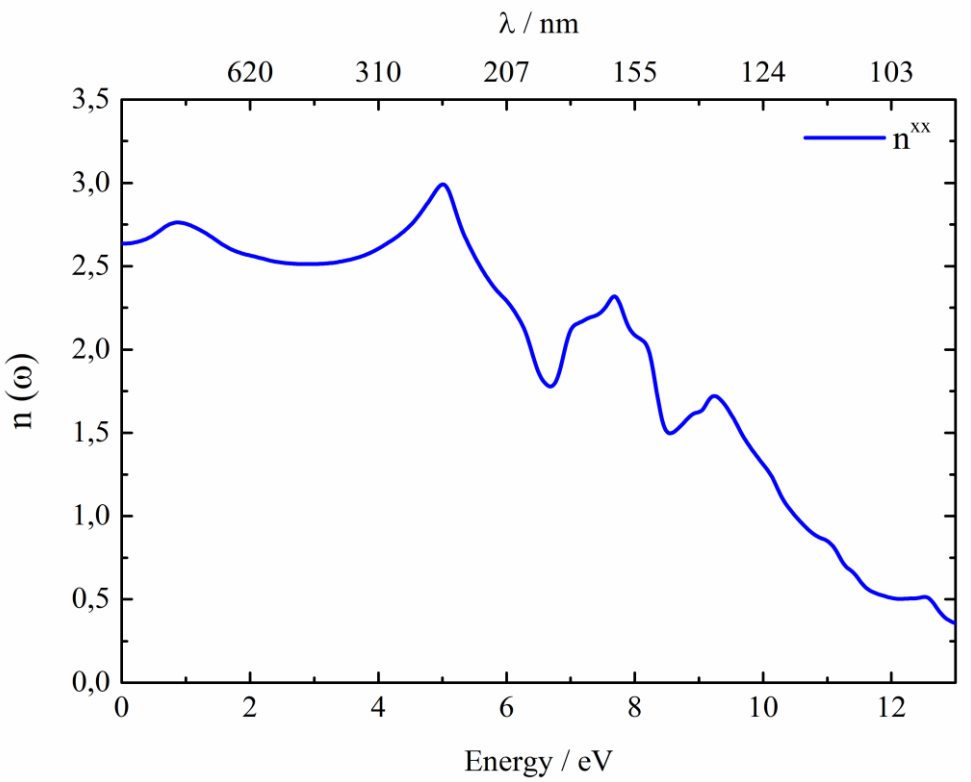

Figure II.9: *The refractive index curve for LiZnN.*

Bibliography:

1. Wood, D., A. Zunger, and R. De Groot, *Electronic structure of filled tetrahedral semiconductors.* Physical Review B, 1985. **31**(4): p. 2570.
2. Carlsson, A., A. Zunger, and D. Wood, *Electronic structure of LiZnN: Interstitial insertion rule.* Physical Review B, 1985. **32**(2): p. 1386.
3. Bacewicz, R. and T. Ciszek, *Preparation and characterization of some AIB II CV type semiconductors.* Applied physics letters, 1988. **52**(14): p. 1150-1151.
4. Wei, S.-H. and A. Zunger, *Electronic structure and phase stability of LiZnAs: A half ionic and half covalent tetrahedral semiconductor.* Physical review letters, 1986. **56**(5): p. 528.
5. Kuriyama, K., T. Kato, and K. Kawada, *Optical band gap of the filled tetrahedral semiconductor LiZnAs.* Physical Review B, 1994. **49**(16): p. 11452.
6. Kuriyama, K., T. Kato, and T. Tanaka, *Optical band gap of the filled tetrahedral semiconductor LiZnN.* Physical Review B, 1994. **49**(7): p. 4511.
7. Beleanu, A., et al., *Systematical, experimental investigations on LiMgZ (Z= P, As, Sb) wide band gap semiconductors.* Journal of Physics D: Applied Physics, 2011. **44**(47): p. 475302.
8. Madsen, G.K., *Automated search for new thermoelectric materials: the case of LiZnSb.* Journal of the American Chemical Society, 2006. **128**(37): p. 12140-12146.
9. Nowotny, H. and W. Sibert, *Ternäre Valenzverbindungen in den Systemen Kupfer (Silber)-Arsen (Antimon, Wismut)-Magnesium.* Z. Metallkd, 1941. **33**: p. 391-394.
10. Juza, R. and F. Hund, *Die ternären Nitride LiMgN und LiZnN. 16. Mitteilung über Metallamide und Metallnitride.* Zeitschrift für anorganische Chemie, 1948. **257**(1-3): p. 1-12.
11. Nowotny, H. and K. Bachmayer, *Ternäre Valenzverbindungen vom Flußspattyp.* Monatshefte für Chemie/Chemical Monthly, 1949. **80**(5): p. 734-734.
12. Juza, R., K. Langer, and K. Von Benda, *Ternary nitrides, phosphides, and arsenides of lithium.* Angewandte Chemie International Edition in English, 1968. **7**(5): p. 360-370.
13. Rompa, H., M. Schuurmans, and F. Williams, *Predicted modifications in the direct and indirect gaps of tetrahedral semiconductors.* Physical review letters, 1984. **52**(8): p. 675.

14. Obot, I., D. Macdonald, and Z. Gasem, *Density functional theory (DFT) as a powerful tool for designing new organic corrosion inhibitors. Part 1: an overview.* Corrosion Science, 2015. **99**: p. 1-30.
15. Blaha, P., et al., *wien2k.* An augmented plane wave+ local orbitals program for calculating crystal properties, 2001.
16. Perdew, J.P., K. Burke, and M. Ernzerhof, *Generalized gradient approximation made simple.* Physical review letters, 1996. **77**(18): p. 3865.
17. Slater, J.C., *The ferromagnetism of nickel.* Physical Review, 1936. **49**(7): p. 537.
18. Kalarasse, F. and B. Bennecer, *Structural and elastic properties of the filled tetrahedral semiconductors LiZnX (X= N, P, and As).* Journal of Physics and Chemistry of Solids, 2006. **67**(4): p. 846-850.
19. Bouhemadou, A., R. Khenata, and F. Zerarga, *Prediction study of elastic properties under pressure effect for filled tetrahedral semiconductors LiZnN, LiZnP and LiZnAs.* Solid state communications, 2007. **141**(5): p. 288-291.
20. Mehl, M.J., *Pressure dependence of the elastic moduli in aluminum-rich Al-Li compounds.* Physical Review B, 1993. **47**(5): p. 2493.
21. Vaitheeswaran, G., et al., *High-pressure structural, elastic, and electronic properties of the scintillator host material K Mg F 3.* Physical Review B, 2007. **76**(1): p. 014107.
22. Young, T., *Miscellaneous Works of the Late Thomas Young*. Vol. 2. 1855: J. Murray.
23. Fu, H., et al., *Ab initio calculations of elastic constants and thermodynamic properties of NiAl under high pressures.* Computational Materials Science, 2008. **44**(2): p. 774-778.
24. Young, A.F., et al., *Synthesis of novel transition metal nitrides IrN 2 and OsN 2.* Physical review letters, 2006. **96**(15): p. 155501.
25. Pugh, S., *XCII. Relations between the elastic moduli and the plastic properties of polycrystalline pure metals.* The London, Edinburgh, and Dublin Philosophical Magazine and Journal of Science, 1954. **45**(367): p. 823-843.
26. Frantsevich, I., F. Voronov, and S. Bokuta, *Elastic Constants and Elastic Moduli of Metals and Insulators, ed. IN Frantsevich*, 1983, Naukova Dumka, Kiev.
27. Dragomir, I. and T. Ungár, *The dislocations contrast factors of cubic crystals in the Zener constant range between zero and unity.* Powder Diffraction, 2002. **17**(2): p. 104-111.
28. Ueda, K., et al., *Epitaxial growth of transparent p-type conducting CuGaO 2 thin films on sapphire (001) substrates by pulsed laser deposition.* Journal of applied physics, 2001. **89**(3): p. 1790-1793.

29. Boukortt, A., et al., *First-principle calculation of the optical properties of zinc-blende Zn1− xCdxSySe1− y.* Physica B: Condensed Matter, 2010. **405**(2): p. 763-769.
30. Berrah, S., A. Boukortt, and H. Abid, *Optical properties of the cubic alloy (In, Ga) N.* Physica E: Low-dimensional Systems and Nanostructures, 2009. **41**(4): p. 701-704.
31. Teng, D., et al., *Effects of ordering on the band structure of III–V semiconductors.* Journal of Physics and Chemistry of Solids, 1991. **52**(9): p. 1109-1128.
32. Bennacer, H., et al., *Electronic and optical properties of GaInX 2 (X= As, P) from first principles study.* 2015.
33. Lee, K.-H., S.-G. Lee, and K.-J. Chang, *Optical properties of ordered In 0.5 Ga 0.5 P alloys.* Physical Review B, 1995. **52**(22): p. 15862.
34. Van Deelen, J., et al., *On the development of high-efficiency thin-film GaAs and GaInP2 cells.* Journal of crystal growth, 2007. **298**: p. 772-776.
35. Schubert, M., et al., *Direct-gap reduction and valence-band splitting of ordered indirect-gap AlIn P 2 studied by dark-field spectroscopy.* Physical Review B, 1996. **54**(24): p. 17616.
36. Kozhevnikov, M., et al., *Evolution of GaAs 1− x N x conduction states and giant A u/G a A s 1− x N x Schottky barrier reduction studied by ballistic electron emission spectroscopy.* Physical Review B, 2000. **61**(12): p. R7861.
37. Callahan, A.A.A., *Other means of communication*, 2013, Massachusetts Institute of Technology.
38. Goldhahn, R., et al., *Determination of Optical Constants for Cubic InxGa1—xN Layers.* physica status solidi (b), 1999. **216**(1): p. 265-268.

General Conclusion

General Conclusion:

The structural, electronic ,elastic and optical properties of the half-Heusler semiconductor compound LiZnN have been investigated in this work, by using full-potential linear-augmented plane wave (FP-LAPW) method formed within the density functional theory DFT. Generalized gradient approximation (GGA) was used to calculate the exchange correlation energy and potential.

Our theoretical and study can be summarized as follows:

- **Structural properties:**

First, we studied the structural properties in order to characterize the fundamental state of the studied system. Three possible differerent types were investigated where, the results of structural optimization of LiZnN show that our compound is more stable in the phase NM type I.

- **Elastic properties:**

Second, the computed elastic properties indicate the stability of our compound. The value of B/G ratio has been found to be 1.35, which shows that our compound is brittle in nature. In addition the Zener anisotropy factor (A) has been calculated and found less than one which indicates the anisotropy characteristic.

- **Electronic properties:**

Next, the electronic properties such as density of states and band structures have been presented. The LiZnN compound shows a direct band gap (Γ- Γ).

- **Optical properties:**

The optical properties such as dielectric function and absorption coefficient, refractive and reflectivity index have been also calculated in order to study the behavior of the semiconductor LiZnN. The real part, Ɛ1 (ω) of the static dielectric function at 0eV for LiZnN is equal to 6.95. this means that the dispersion is zero, and therefore the absorption is maximum. We found that the fundamental absorption threshold starts at approximately 0.53eV; this value

corresponds to the energy gap for LiZnN. Also the reflectivity starts to increase R (0) =.20 eV which corresponds to the IR spectral region, up to the energy value 13 eV which corresponds to the far UV spectral region. This result can be used as a theoretical basis for potential application in optoelectronic and thermoelectric.

Finally, it is worth noting that the WIEN2k code is a very powerful tool which allows easy and direct calculation of the different properties of the matter despite of our modest and short experience of using it.

Abstract:

Structural, elastic, electronic and optical semiconductor compound properties LiZnN have been calculated by the augmented plane waves (FP-LAPW) method based on the theory of the functional of the density (DFT) using the Wien2K code. We used the approximation of generalized gradient GGA for the term of the Exchange and correlation potential. From the elastic properties after it was mechanically stable. The electronic and optical properties are also discussed, according to the calculation of the structure of electronic bands and the density of total states; we found that this compound has a direct gap, with a semiconductor behavior. Which is suitable for thermoelectric and optoelectronic applications. The results in this work appear promising for future experimental investigations.

Keywords: Density functional theory (DFT), generalized gradient functional (GGA), dielectric function, absorption, reflectivity, half-Heusler.

Résumé :

Les propriétés structurelles, élastiques, électroniques et optique du composé semi-conducteur LiZnN ont été calculées par la méthode des ondes planes augmentées (FP-LAPW) qui se base sur la théorie de la fonctionnelle de la densité (DFT) en utilisant le code Wien2K. Nous avons utilisé l'approximation du gradient généralisé GGA pour le terme du potentiel d'échange et de corrélation. D'après les propriétés élastiques il a été constaté que notre matériau est mécaniquement stable. Les propriétés électroniques et optiques sont également discutées, d'après le calcul de la structure de bande électronique et de la densité d'états (DOS), nous avons constaté que ce composé présente un gap direct. Avec un comportement semi-conducteur. Ce qui convient aux application thermoélectriques et optoélectroniques. Les résultats de ces travaux semblent prometteurs pour de futures recherches expérimentales.

Mots-clés: Théorie de le fonctionnelle de la densité (DFT), fonctionnelle du gradient généralisé (GGA), fonction diélectrique, absorption, réflectivité, demi-Heusler.

ملخص

قمنا بدراسة الخصائص الهيكلية و الخصائص المرنة ,الخصائص الالكترونية والضوئية لمركب Half-Heusler LiZnN.تم استخدام طريقة الأمواج المستوية المتزايدة خطيا (LAPW-FP) في إطار نظرية دالة الكثافة (DFT) باستعمال برنامج k2Wien لأجل حساب كمون التبادل الارتباط تم استخدام تقريب التدرج المعمم GGA, الخصائص الهيكلية المحسوبة مثل معامل الشبكة ومعامل الانضغاط كانت موافقة للبيانات التجريبية والنظرية المتاحة دراستنا لخواص المرونة LiZnN تشير ثوابت المرونة التي تم الحصول عليها أن مركب LiZnN مستقر ميكانيكيا . كما تكشف بنية العصابة ان المركب LiZnN هو شبه ناقل ذو فجوة مباشرة من أشباه الموصلات عند النقطة Γ يساوي 0.519 كما قمنا بتحليل الخواص البصرية مثل : دالة العزل الكهربائي, معامل الانكسار , الانعكاسية و معامل الامتصاص.

الكلمات المفتاحية: نظرية الكثافة الوظيفية، دالة التدرج المعمم، وظيفة العزل الكهربائي ،الامتصاص، الانعكاسية، نصف هسلر